Journal of Science and Transport Technology
Journal homepage: https://jstt.vn/index.php/en

Stress-dependent SPT-based estimation of small-strain shear modulus for marine sand in central Vietnam and application to high-speed railway foundations

Dang Hong Lam[1,*], Phi Hong Thinh[1], Tran Khanh Hoan[1], Nguyen Chau Lan[1], Cao Van Doan[2], Do Duc Phi[3]

[1]University of Transport and Communications, No.3 Cau Giay street, Hanoi, Vietnam

[2]Mechanics of Advanced Materials and Structures, University of Transport Technology, Hanoi, Vietnam

[3]Univ. Orléans, Univ. Tours, INSA CVL, Lamé, UR 7494, France

Article info
Type of article:
Original research paper

DOI:
https://doi.org/10.58845/jstt.utt.2026.en.6.5.349-363

***Corresponding author:**
Email address:
Dang.hong.lam@utc.edu.vn

Received: 19/06/2026
Received in Revised Form: 30/09/2026
Accepted: 19/10/2026

Abstract: This study evaluates the influence of effective stress on the small-strain shear modulus (G_0) of coastal sand in central Vietnam using data obtained from downhole seismic and standard penetration tests (SPT). A database consisting of 50 paired SPT–downhole test intervals collected from the investigated boreholes was analyzed to develop a stress-dependent correlation of the form $G_0 = A(\sigma'_v)^m N^n$, where G_0 is expressed in MPa and $\sigma'v$ in kPa. Regression analysis indicates that the contribution of SPT resistance ($n \approx 0.40$) is substantially greater than that of effective stress ($m \approx 0.20$), suggesting that soil shear stiffness is governed primarily by penetration resistance. The weak stress dependency explains why conventional G_0–N correlations provide reasonable predictions for the investigated deposits. The proposed formulation offers a practical framework for preliminary stiffness estimation and dynamic behavior assessment of coastal sandy soils under field conditions. To demonstrate its engineering applicability, the estimated G_0 profiles were incorporated into a layered elastic railway foundation model based on the analytical approach proposed by Sheng et al. (1999). Representative loading conditions corresponding to the future North–South High-Speed Railway in Vietnam, including passenger and freight axle loads, were considered. Parametric analyses were conducted to evaluate the effects of train speed, and axle load on the vertical displacement response of the foundation system. The results indicate that the proposed correlation can provide realistic stiffness profiles for preliminary evaluation of railway foundation performance and can serve as a practical tool for geotechnical assessment in regions where direct geophysical measurements are unavailable.

Keywords: marine sand, small-strain shear modulus, SPT resistance, effective stress, high-speed railway, vertical displacement.

1. Introduction

The small-strain shear modulus (G_0) is a fundamental parameter in geotechnical engineering because it governs the wave

propagation characteristics and settlement of soils under static and dynamic loading. Reliable estimation of G_0 is important for foundation design, seismic analysis, and railway vibration assessment.

Despite its importance in the analysis and prediction of railway-induced ground vibration and deformation, direct measurements of G_0 using geophysical methods such as cross-hole, downhole, seismic CPT, or surface-wave testing are rarely available in routine geotechnical investigations. In contrast, SPT N-values are commonly obtained during site characterization and constitute one of the most widely available sources of subsurface information. Therefore, developing a reliable correlation between SPT measurements and G_0 is of practical importance, as it enables advanced analytical models requiring stiffness parameters to be applied using conventional geotechnical investigation data.

Numerous empirical relationships have been proposed to estimate small-strain stiffness from SPT data. Early studies by [1-2] demonstrated that soil stiffness is influenced by stress state, density, and soil fabric. Subsequently, several studies [3-5] proposed correlations linking G_0 or shear-wave velocity to SPT resistance. More recently, an updated SPT-based correlation using a large database was presented by [6]. Although these studies demonstrated the usefulness of SPT-based estimation methods, most practical correlations primarily rely on penetration resistance and do not explicitly consider the contribution of effective stress. Hardin-type formulations and later developments by [7] highlighted the influence of density and stress state; however, their applicability to marine sand deposits remains insufficiently investigated.

For sand soils, effective stress is generally recognized as an important factor controlling interparticle contact stiffness and, consequently, small-strain stiffness. Nevertheless, the relative importance of effective stress compared with penetration resistance remains uncertain, particularly for marine sand deposits. Furthermore, experimental data for coastal marine sands in Vietnam remain limited, despite the increasing demand for reliable stiffness parameters in transportation infrastructure projects.

The ongoing development of the North–South High-Speed Railway in Vietnam has created a need for practical methods to estimate soil stiffness parameters required for vibration and deformation analyses and predictions [8]. Especially, reliable estimation of G_0 is particularly important because this parameter serves as a key input for analytical and numerical modelling of railway-induced ground settlement. In Vietnam, large SPT datasets from many projects are available, whereas direct geophysical measurements are not. Therefore, practical methods for deriving G_0 from routine site investigation data are extremely useful and can facilitate preliminary assessments of high-speed railway foundations.

This study investigates the relationship between small-strain shear modulus, SPT resistance, and effective stress using downhole seismic and SPT data collected from marine sand deposits in Quang Tri Province, central Vietnam. The objectives are multiple: (1) to investigate and develop a stress-dependent correlation for estimating G_0 from SPT data; (2) to evaluate the relative contributions of penetration resistance and effective stress to small-strain stiffness; and (3) to examine the applicability of the estimated stiffness profiles in the analytical assessment of high-speed railway foundation response.

2. Database and Methodology

2.1. Geological conditions

The study area is in Quang Tri Province, central Vietnam, where the subsurface conditions are dominated by marine sand deposits formed under coastal depositional environments. These deposits mainly consist of sandy soils with varying degrees of density and are typical of coastal plains

in central Vietnam. A comprehensive geotechnical investigation was conducted at the site, including 50 boreholes (Fig.1). Standard penetration tests were performed at regular depth intervals, providing a consistent dataset for evaluating the stiffness characteristics of the soil.

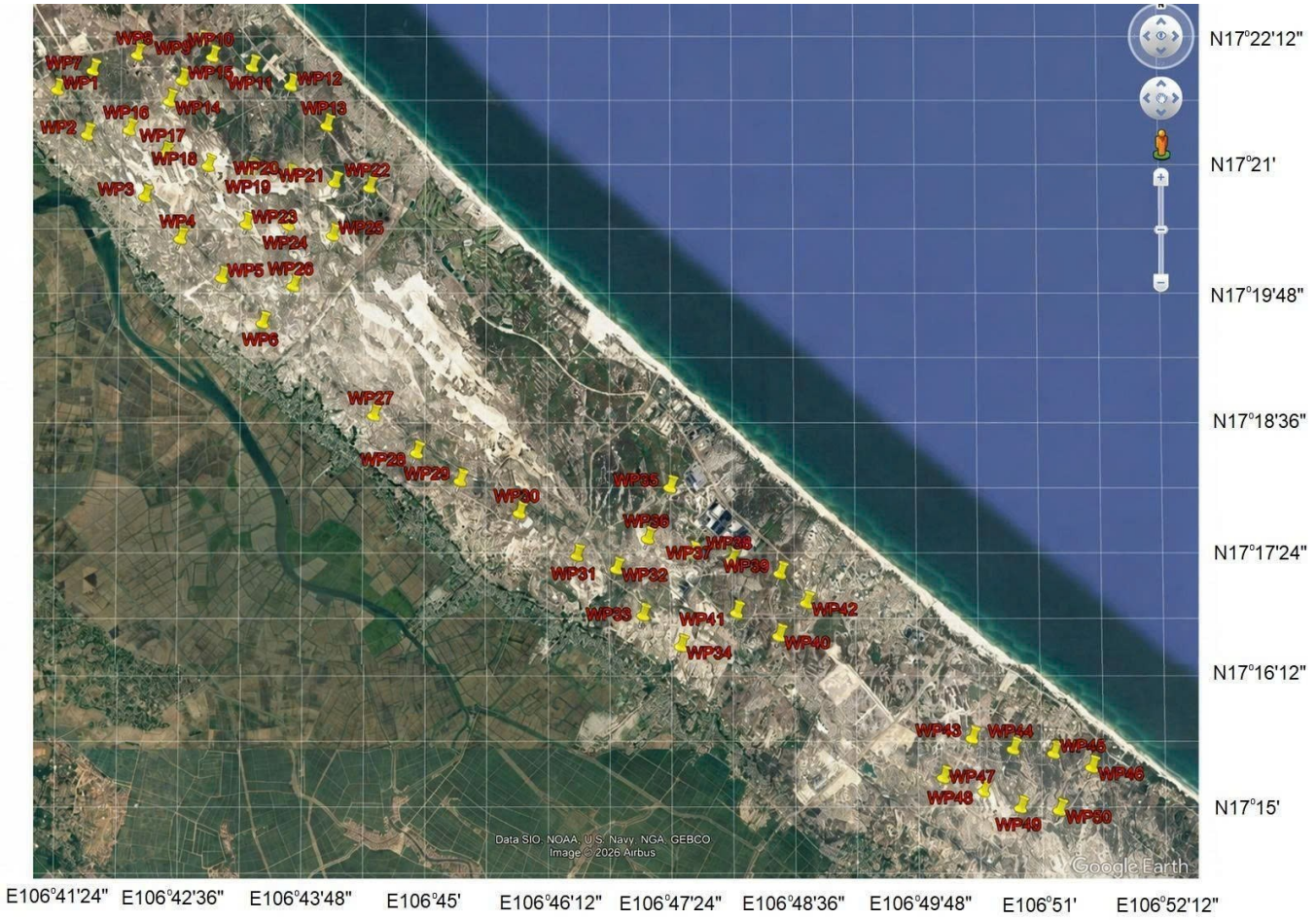


Fig. 1. Location and distribution of the 50 boreholes in the study area

Table 1. Grain size distribution of marine sand in Quang Tri Province

Item	Grain size: Cumulative percentage finer (%)				Effective size (mm)		
	Clay	Silt	Sand	Gravel	D_{10}	D_{30}	D_{60}
Minimum	-	5	95	-	0.1	0.2	0.3
Maximum	-	0	100	-	0.2	0.3	0.5

The investigated sand is typically fine to medium in grain size and is generally saturated due to the shallow groundwater table commonly observed in coastal areas. The marine origin of the deposits results in weak cementation and a relatively loose structure, particularly in the upper layers. As the main purpose, the analysis conducted in this work focuses on sand layers represented in the database, covering a depth range of approximately 2 to 30.7 m. The corresponding SPT resistance values range from 8 to 76, as summarized in Table 2. Within this range, the variation in effective vertical stress is relatively moderate.

Table 1 summarizes the grain size distribution characteristics of the investigated sand according to ASTM standards [9-10]. The results indicate that the soil is predominantly sandy, with sand content ranging from approximately 95% to 100%, and negligible amounts of clay and gravel fractions.

The effective grain sizes (D_{10} = 0.1 - 0.2 mm,

D_{30} = 0.2 - 0.3 mm, and D_{60} = 0.3 - 0.5 mm) suggest a relatively uniform to moderately graded sand. Such grain size characteristics are typical of young marine deposits and are associated with loose to medium dense soil states.

2.2. Database of small-strain shear modulus

The small-strain shear modulus (G_0) was obtained from downhole seismic tests [11], providing reliable measurements of in-situ stiffness at very small strain levels.

The downhole seismic test setup used in this study is illustrated in Fig. 2. The system consists of a seismic source, a downhole geophone, and a data acquisition unit. As shown in Fig. 2(a), the equipment includes a multi-channel seismograph connected to a cable reel and a triaxial geophone for recording wave signals [12]. Fig. 2(b) presents the field implementation of the test, where seismic waves are generated at the ground surface and recorded at various depths within the borehole. The setup demonstrates typical field conditions, including sensor installation, cable connections, and data acquisition procedures.

The combined use of controlled wave generation and in situ measurement enables reliable determination of shear wave velocity (V_s), which serves as the basis for evaluating the small-strain shear modulus (G_0) in this study.

The small-strain shear modulus (G_0) was derived from shear wave velocity (V_s) measurements obtained from downhole seismic tests. The relationship between G_0 and V_s is given by Eq. (1)

$$G_0 = \rho V_s^2 \quad (1)$$

where ρ is the mass density of the soil and V_s is the shear wave velocity. The mass density was estimated based on typical unit weight values of saturated marine sand.

Based on laboratory measurements of bulk density (ρ = 1.90÷2.07 g/cm³), a representative value of ρ = 1.90 g/cm³ was adopted to convert shear wave velocity-based correlations into the small-strain shear modulus using the elastic relationship given in Eq. (1).

Standard penetration tests were performed at corresponding depths to determine penetration resistance (N-values). The depth of the paired SPT–downhole test intervals used in the regression analysis ranges from approximately 4 to 30.7 m, covering the representative sand deposits included in the database.



(a) (b)

Fig. 2. Downhole seismic test setup: (a) equipment components including seismograph and geophones; (b) field implementation at the borehole location.

The combination of downhole seismic data and SPT results allows for a consistent evaluation of the relationship between small-strain stiffness and penetration resistance. The dataset also

provides a basis for examining the influence of stress conditions on the stiffness characteristics of marine sand (Table 2).

As shown in Fig. 3, G_0 increases consistently with N-value, confirming that penetration resistance plays a dominant role in controlling small-strain stiffness. In contrast, Fig. 4 shows that G_0 does not exhibit a strong correlation with depth, suggesting a limited influence of effective stress.

2.3. Methodology

Table 2. Statistical analysis of database

Parameter	Min	Max	Mean	S_{td}
Depth (m)	2	30.7	12.08	6.18
SPT N (-)	8	76	37.38	15.47
G_0 (MPa)	64.18	363.93	169.72	72.18

where S_{td} is the standard deviation

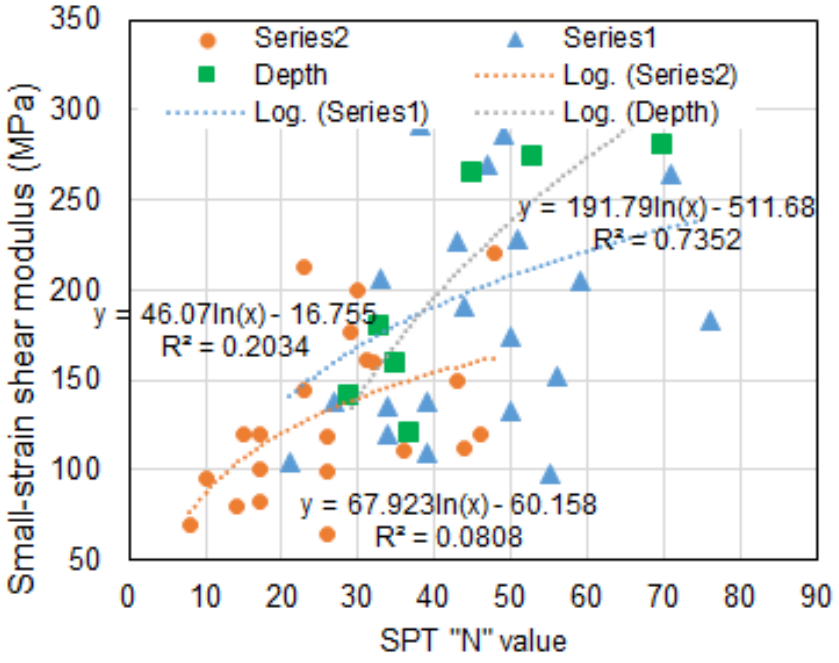


Fig. 3. Relationship between small-strain shear modulus (G_0) and SPT resistance (N).

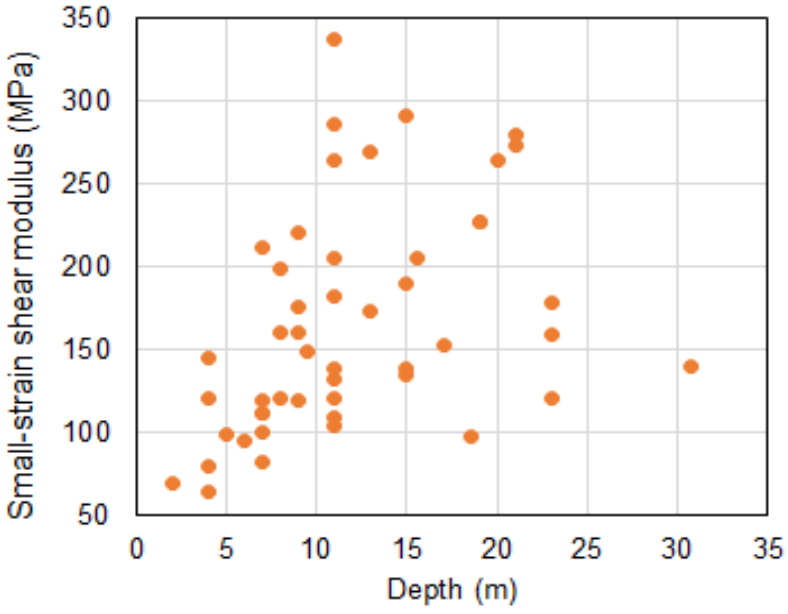


Fig. 4. Variation of G_0 with depth (as a proxy for effective stress).

As discussed in [1-2], small-strain shear modulus is governed not only by penetration resistance and effective stress, but also by void ratio characteristics. In addition to SPT resistance, several studies have emphasized the role of effective stress in controlling soil stiffness. Based on theoretical considerations and experimental observations, the small-strain shear modulus is often expressed in the form of Eq. (2)

$$G_0 = A(\sigma'_v)^m f(\text{density}) \quad (2)$$

where σ'_v is the effective vertical stress and the exponent m typically ranges from 0.2 to 0.5 for sand soils. This formulation reflects the influence of confining stress on interparticle contact stiffness. A practical value of m equal to 0.25 was proposed by [7], while a value of A equal to 51 is given in [1] for round-grained Ottawa sand, and f(density) = 2.17-e; However, in practical applications, the density term is often represented indirectly through SPT resistance, leading to combined empirical models written in the following form:

$$G_0 = A(\sigma'_v)^m N^n \quad (3)$$

In Eq. (3), G_0 is expressed in MPa, σ'_v is expressed in kPa, and N is dimensionless. Accordingly, the coefficient A is unit-dependent, and its value is valid only for the above unit convention, whereas the exponents m and n are dimensionless.

To determine the model parameters, a logarithmic transformation was applied to linearize the previous Eq. (3) in the following form:

$$\ln G_0 = \ln A + m\ln\sigma'_v + n\ln N \quad (4)$$

Multiple linear regression analysis was then performed using the experimental dataset. This approach allows for the quantitative evaluation of the relative contributions of SPT resistance and effective stress to small-strain stiffness.

In addition, the performance of the stress-dependent model was compared with conventional SPT-based correlations to assess whether the inclusion of effective stress significantly improves the prediction of G_0 for marine sand deposits.

3. Results and discussion

3.1. Stress-dependent correlation of small-strain shear modulus

The regression analysis based on the experimental dataset yielded the following stress-dependent relationship between the small-strain shear modulus, SPT resistance, and effective stress:

$$G_0 = 15.8(\sigma'_v)^{0.20} N^{0.40} \quad (5)$$

The moderate coefficient of determination ($R^2 \approx 0.39$) reflects the inherent scatter associated with empirical correlations between SPT resistance and small-strain shear modulus. Such scatter is also observed in previously published G_0–N correlations, as summarized in Table 3.

Table 3. Regression results of this study in comparison with the previous contributions in the literature

No	References	Formula (*)	SEE	PCC
1	[1-2]	V_s=A f(density) $(\sigma'_v)^m$	0.425	0.453
2	[3]	$G_0 = 13.63N^{0.72}$	0.311	0.571
3	[4]	$G_0 = 17.36N^{0.631}$	0.328	0.573
4	[5]	$G_0 = 6.22N$	0.363	0.561
5	[6]	$G_0 = 24.28N^{0.55}$	0.314	0.575
6	This study	$G_0 = 15.8N^{0.4}(\sigma'_v)^{0.2}$	0.298	0.600

Note: SEE: Standard error of estimate; PCC: Pearson correlation coefficient

The proposed correlation nevertheless provides an improved statistical performance, particularly in terms of the standard error of estimate (SEE), while maintaining a comparable Pearson correlation coefficient (PCC) to the existing correlations. The remaining scatter may be attributed to variations in soil fabric, fines content, mineralogical characteristics, groundwater

conditions, and SPT testing and energy-transfer effects, which are not explicitly incorporated into the proposed formulation. Therefore, the proposed relationship should be regarded as a practical empirical correlation for indicative estimation of G_0, rather than as an exact deterministic prediction.

The obtained exponents show that the contribution of N-value (n ≈ 0.40) is significantly greater than that of effective stress (m ≈ 0.20) (Table 3). This result suggests that penetration resistance plays a dominant role in controlling the small-strain stiffness of the investigated sand, while the influence of effective stress is comparatively limited.

3.2. Role of effective stress

Effective stress is generally considered an important factor influencing soil stiffness, because it reflects the stress state of soil deposits. However, the relatively small exponent associated with effective stress in the present study indicates that its contribution to small-strain shear modulus is less significant than commonly assumed. This observation may be attributed to the geological characteristics of the investigated deposits. The study area is covered by young Holocene marine deposits (mvQIV³), consisting mainly of quartz sand interbedded with silt and clay containing organic matter, with a thickness ranging from 2 to 15 m. Under such conditions, the stiffness of the soil may be more strongly governed by particle arrangement and density, which are captured by SPT resistance, rather than by confining stress.

The results are consistent with the observed scatter in the experimental data, where variations in G_0 are more closely related to changes in SPT N-values than to depth or stress level. These finding highlights that, for young marine sand deposits, the role of effective stress in stiffness estimation may be secondary.

From a micromechanical point of view, the small-strain shear modulus of sand soils is governed by interparticle contact stiffness and coordination number. Effective stress influences G_0 by increasing the normal force at particle contacts, thereby enhancing contact stiffness.

However, for relatively loose and young sandy deposits, the coordination number and particle arrangement may play a more dominant role than confining stress. In such cases, parameters related to soil density and fabric, which are indirectly captured by SPT resistance, become the primary controlling factors.

This explains why the exponent associated with effective stress in the present study is relatively small, and why G_0 is more sensitive to *N*-value than to stress level.

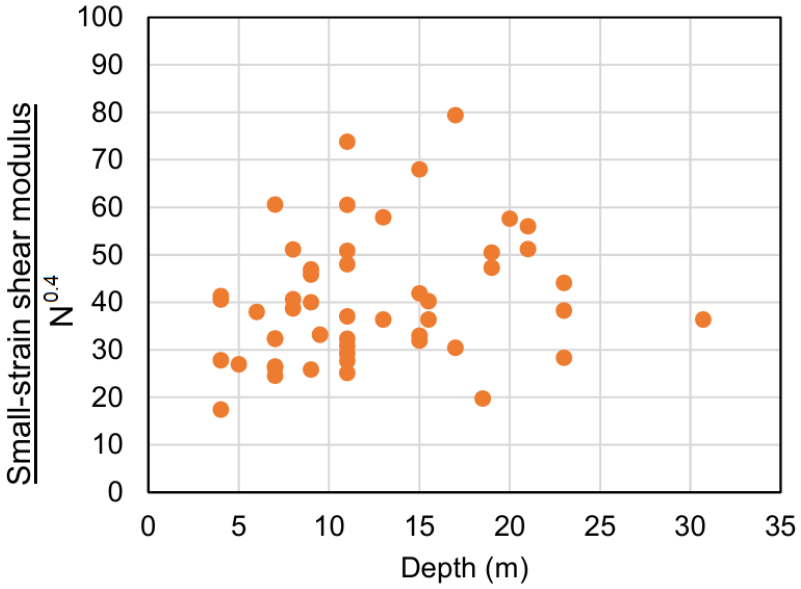


Fig. 5. Normalized shear modulus ($G_0/N^{0.4}$) versus depth.

The normalized results $G_0 / N^{0.40}$ (Fig. 5) further confirm that once the effect of N-value is accounted for, the influence of effective stress becomes negligible.

3.3. Comparison with conventional correlations

To assess the practical significance of the proposed model, the results were compared with conventional empirical correlations based solely on SPT resistance. These correlations typically take the form of Eq. (6)

$$G_0 = aN^b \quad (6)$$

where the parameters a and b are obtained from regression analysis.

The comparison shows that conventional G_0–N relationships provide predictions that are generally comparable to those obtained from the stress-dependent model. This can be explained by the relatively limited contribution of effective stress observed in the present study.

Therefore, the inclusion of effective stress in the model does not significantly improve the predictive capability for the investigated dataset. Instead, SPT-based correlations remain an effective and practical approach for estimating small-strain shear modulus of marine sand in the study area.

As shown in Fig. 6, the predictions from the conventional G_0–N model are comparable to those obtained from the proposed stress-dependent formulation (Eq.5). Both approaches exhibit similar scatter around the 1:1 line, indicating that the inclusion of effective stress does not significantly improve predictive performance.

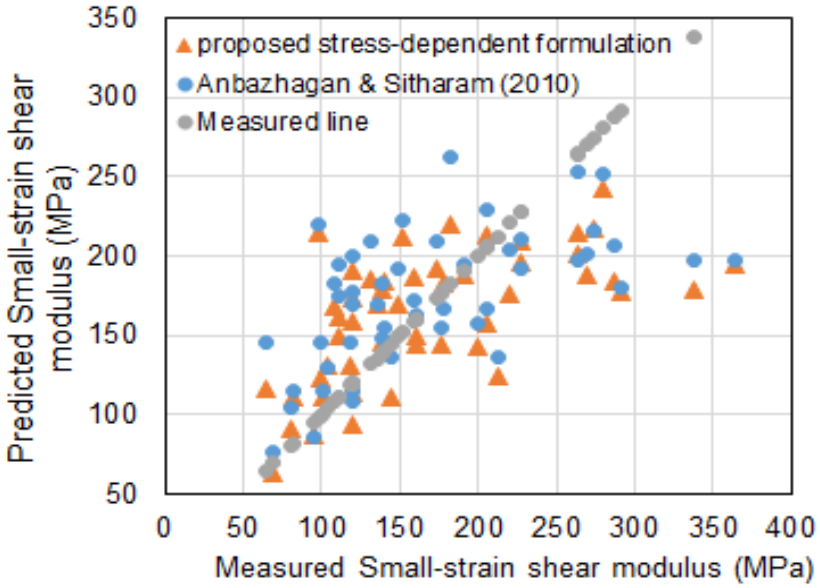


Fig. 6. Comparison between measured and predicted small-strain shear modulus using the conventional G_0–N correlation and a stress-dependent model.

3.4. Implications of groundwater fluctuation on G_0 estimation

Groundwater fluctuation may affect the estimation of small-strain shear modulus (G_0), especially in coastal areas with seasonal groundwater variations. In this study, the sand layers are assumed to be fully saturated, and effective stress is calculated using a constant submerged unit weight.

In coastal regions such as Quang Tri Province, seasonal rainfall and tidal effects may cause noticeable groundwater variations. However, due to the weak stress dependency of the proposed model, a groundwater fluctuation of about 5 m results in only a small variation in G_0 (approximately 5–10%). Fig. 7 shows that the influence of SPT N-value on G_0 is much greater than that of groundwater fluctuation, indicating that penetration resistance is the dominant factor controlling small-strain stiffness.

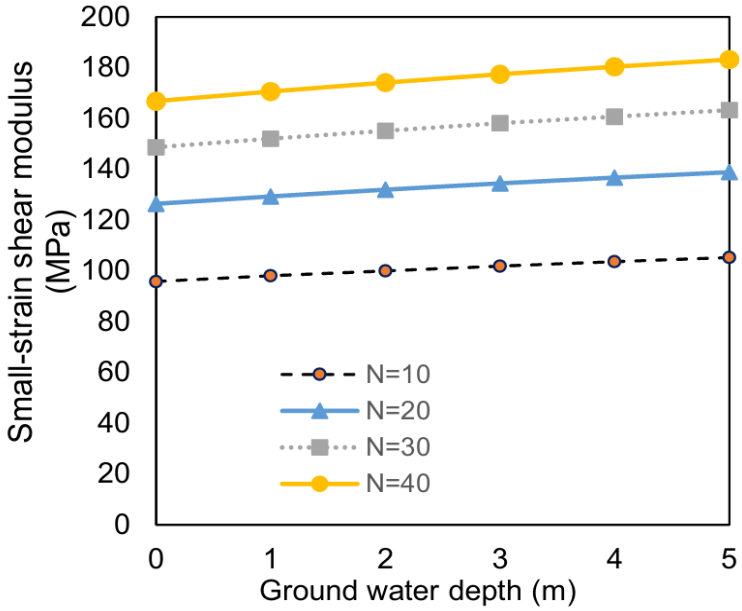


Fig. 7. Influence of groundwater depth on small-strain shear modulus (G_0) for different SPT N-values.

3.5. Engineering Application to High-Speed Railway Foundations

From a practical perspective, the results of this study suggest that SPT-based correlations can be used with reasonable accuracy for estimating the small-strain shear modulus of marine sand without explicitly incorporating effective stress. This finding is particularly useful for engineering applications where detailed stress information is not readily available or where rapid estimation is required. The use of simplified G_0–N relationships can significantly reduce the effort required for data processing while still providing reliable estimates for preliminary design and analysis

However, it should be noted that the conclusions of this study are based on a specific dataset of marine sand in central Vietnam. For other soil types or geological conditions, the influence of effective stress may differ and should be evaluated accordingly

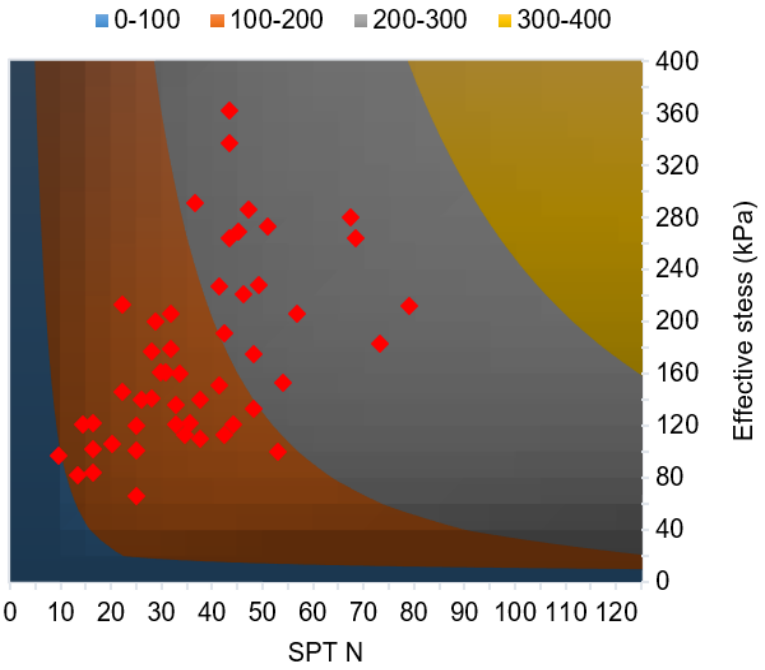


Fig. 8. Contour plot of small-strain shear modulus (G_0) as a function of SPT N-value and effective stress (σ'_v) based on the proposed model. Red markers represent measured field data.

The contour plot in Fig. 8 illustrates the combined influence of N-value and effective stress on G_0. It can be observed that the contour lines are more closely spaced along the *N*-direction, indicating a stronger sensitivity of G_0 to SPT N-value compared to effective stress.

3.5.1. Small-strain shear modulus of typical borehole log in Quang Tri site

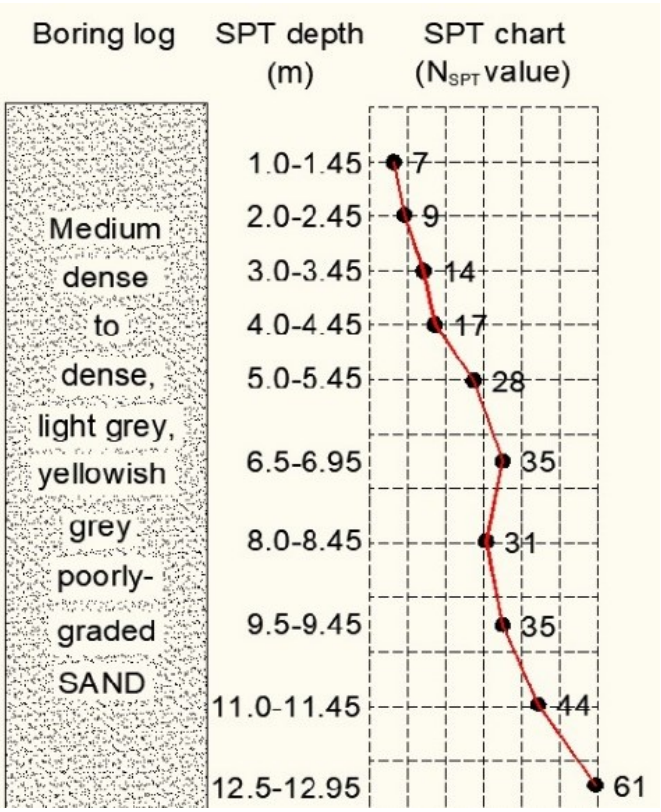


Fig. 9. Representative borehole profile and variation of SPT N-value with depth at the study site

Table 4. Estimated small-strain shear modulus (G_0) profile and selected representative values for layered ground modelling

Depth	SPT	σ'v	G_0	Selected average G_0
(m)		kPa	MPa	MPa
1	7	8.2	52	
2	9	16.4	67	
3	14	24.6	86	85
4	17	32.8	99	
5	28	41	126	
6	35	49.2	143	
7	35	57.4	147	
8	31	65.6	144	150
9	35	73.8	155	
10	35	82	158	
11	44	90.2	177	
12	61	98.4	205	
13	61	106.6	208	200
14	61	114.8	211	
15	61	123	214	

Based on the representative borehole profile shown in Fig. 9 and the proposed correlation presented in Eq. (5), the small-strain shear modulus (G_0) was estimated at different depths using the measured SPT N-values and effective overburden stress. The calculated G_0 profile is summarized in Table 4.

To facilitate subsequent engineering analyses and reduce the complexity associated with layer-by-layer variations, representative average G_0 values were selected for each 5 m soil interval. These averaged values were then used to define the stiffness profile of the layered ground model in the analytical evaluation of railway-induced ground response.

Although several railway studies have employed linear-elastic stiffness in analyses of train-induced railway ground response [13,14], other studies have demonstrated the effects of strain-dependent stiffness degradation on railway dynamic response [15–17]. In the present study, G_0 is used as a reference stiffness parameter to compare the calculated vertical displacement response under different train-speed conditions and to identify the critical train-speed condition, rather than to predict absolute operational or design displacement. The effects of strain-dependent stiffness degradation are therefore not explicitly incorporated in this preliminary assessment and will be considered in subsequent nonlinear analyses.

3.5.2. Analytical Evaluation of Railway-Induced Ground Response

The analytical framework was selected because it explicitly accounts for layered ground stiffness while requiring relatively limited input parameters, making it suitable for preliminary assessments based on routine geotechnical investigation data. The dynamic response of the railway foundation was evaluated using the analytical framework proposed by [18]. In this approach, the railway track is represented by a coupled rail–sleeper–ballast system resting on a layered elastic ground, while the train loading is simplified as a stationary harmonic excitation acting on the rail. This assumption enables efficient investigation of the influence of ground stiffness parameters on vibration propagation and displacement response.

In this study, the reference axle loads adopted are 17 tons/axle for passenger trains operating at speeds up to 350 km/h [8] and 22.5 tons/axle for freight trains operating at speeds up to 150 km/h. These axle loads are represented by equivalent vertical loads acting through the track structure. The objective is not to simulate the complete vehicle–track interaction, but rather to investigate how variations in the small-strain shear modulus (G_0), estimated from SPT N-values, affect the stiffness profile and the resulting vertical displacement response of the layered ground.

Following [18], the railway track is idealized as an Euler beam supported by rail pads, sleepers, and ballast, while the ground is represented as horizontally layered elastic media overlying a half-space. This approach allows the influence of soil stiffness, layer thickness, and wave propagation characteristics to be evaluated efficiently while maintaining reasonable computational effort.

In the present application, the small-strain shear modulus (G_0) profile was first estimated from the proposed SPT-based correlation. The corresponding equivalent Young's modulus (E_0) profile was then derived and used as input for the layered elastic analysis. The resulting vertical displacement distribution was subsequently evaluated under the representative axle load condition to assess the influence of soil stiffness on the performance of the railway foundation system.

The railway foundation system considered in this study is based on the typical ballastless track structure proposed for the Vietnamese North–South High-Speed Railway, as illustrated in Fig. 10. The foundation is idealized as a five-layer system consisting of engineered trackbed materials overlying natural soil deposits.

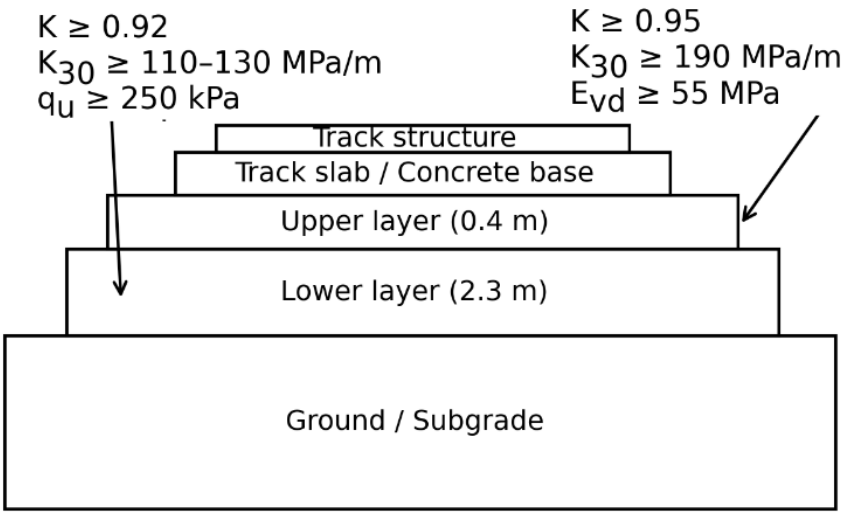


Fig. 10. Simplified ballastless track embankment and layered foundation system adopted for the North–South High-Speed Railway in Vietnam.

The uppermost layer comprises a graded crushed-stone subbase with a thickness of 0.4 m, a unit weight of 22 kN/m³, a dynamic Young's modulus of 150 MPa, and a Poisson's ratio of 0.25. Beneath this layer, a 2.3 m thick compacted fill layer is adopted as the lower subbase, characterized by a unit weight of 20 kN/m³, a dynamic Young's modulus of 100 MPa, and a Poisson's ratio of 0.30 [19].

For the natural soil layers, the small-strain shear modulus (G_0) was estimated using the proposed correlation developed in this study to obtain the values presented in Table 4, while the corresponding equivalent Young's modulus values were subsequently derived and used in the layered elastic analysis.

3.5.3. Computed vertical displacement of typical borehole log in Quang Tri site

To investigate the influence of train speed on the dynamic response of the railway foundation, a series of analytical simulations were performed using the layered elastic model under a constant axle load of 17 tons.

According to the typical bogie wheelbase of approximately 2.5 m, the characteristic excitation frequency generated by a train travelling at 350 km/h is approximately 39 Hz, which is close to the 40 Hz harmonic excitation adopted by [18]. Therefore, the analytical framework was considered appropriate for investigating the dynamic response of the railway foundation under high-speed train loading.

Five representative train speeds (50, 150, 250, 300 and 350 km/h) were considered. To investigate the influence of train speed under identical geological conditions, the estimated small-strain shear modulus (G_0) profile was adopted as the input parameter for the analytical calculations.

Fig. 11 presents the resulting vertical displacement profiles with depth. The calculated vertical displacement response includes the engineered foundation layers (upper and lower base) as well as the underlying natural soil layers. The results indicate that train speed significantly affects the distribution and magnitude of ground displacement, with the largest deformation concentrated within the upper subgrade layers. The influence of train loading decreases rapidly with depth, becoming negligible below the reinforced foundation zone.

The non-monotonic relationship between train speed and vertical displacement (or settlement) indicates that the dynamic response is governed not only by axle load magnitude but also by the interaction between excitation frequency and the natural characteristics of the layered ground system. Under the investigated conditions,

the excitation frequency associated with 250 km/h appears to be closer to the dominant response

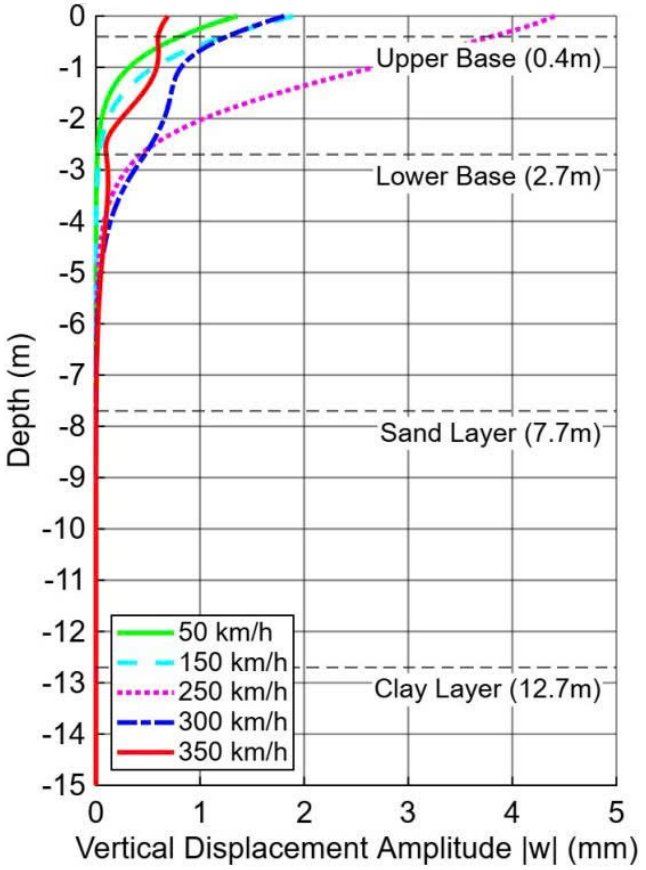


Fig. 11. Effect of train speed on vertical displacement (17 tons/axle load)

Similarly, the influence of train speed was investigated under a freight axle load of 22.5 tons, which represents the design loading condition for future freight operations on the North–South Railway. Three representative train speeds of 50, 100, and 150 km/h were considered while maintaining identical ground conditions and stiffness parameters. The resulting vertical displacement profiles presented in Fig. 12 show that the influence of train speed on the dynamic response in this load is smaller than in the previous case.

Based on the displacement profiles shown in Figs. 11 and 12, the most critical loading conditions correspond to a passenger train with a 17-ton axle load travelling at 250 km/h and a freight train with a 22.5-ton axle load travelling at 150 km/h.

frequency of the foundation system, resulting in larger displacement amplitudes.

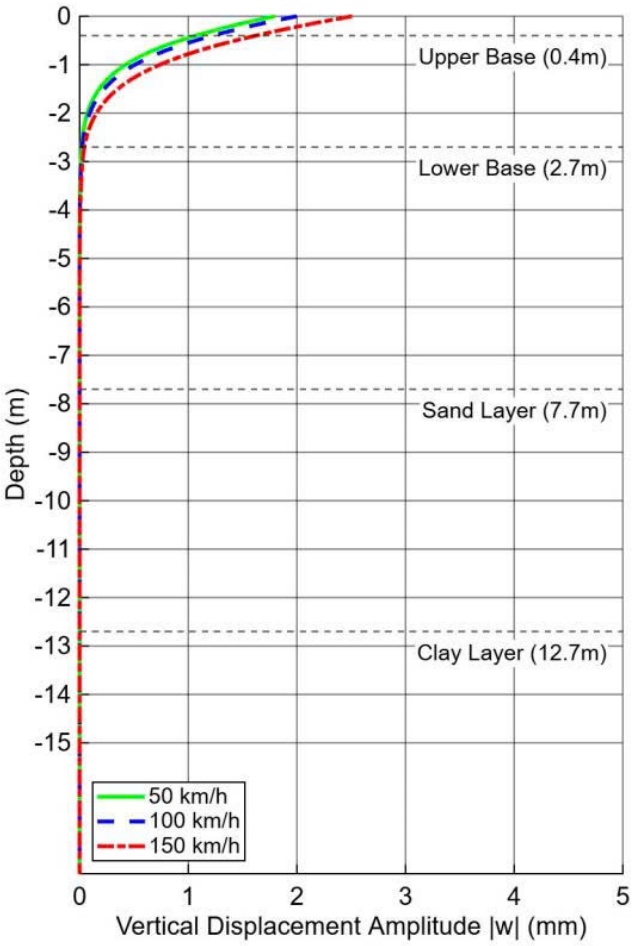


Fig. 12. Effect of train speed on vertical displacement (22.5 tons/axle load)

4. Conclusions

This study evaluated the relative influence of effective stress and SPT resistance on the small-strain shear modulus of coastal sand in central Vietnam using downhole seismic data from 50 test intervals.

A stress-dependent correlation expressed in the power-law form $G_0 = 15.8(\sigma'_v)^{0.20}N^{0.40}$ was developed. The results indicate that penetration resistance plays a dominant role in controlling soil stiffness, whereas the contribution of effective stress is comparatively limited.

Because of the weak stress dependency observed in the investigated deposits, conventional G_0–N correlations provide prediction accuracy

comparable to that of the proposed model. Therefore, simplified SPT-based approaches remain suitable for preliminary stiffness estimation and dynamic assessment of similar coastal sandy soils.

To demonstrate the engineering applicability of the proposed correlation, the estimated (G_0) profiles were incorporated into a layered elastic railway foundation model based on the analytical framework of Sheng et al. (1999). The results demonstrate that both train speed and axle load have a significant influence on the predicted vertical displacement response, highlighting the importance of considering dynamic loading characteristics in the preliminary assessment of railway foundations.

The findings in this work contribute to improving the understanding of stiffness characteristics of Vietnamese marine sand and provide a practical framework for deriving soil stiffness profiles from conventional site investigation data. The proposed approach can support preliminary geotechnical assessment and vertical displacement analysis of high-speed railway foundations in areas where direct measurements of small-strain stiffness are not available. Although the investigated site in Quang Tri Province represents a typical coastal marine sand setting in central Vietnam, localized site investigation is recommended to verify the applicability of the proposed correlation to other geographical and geological conditions.

Acknowledgments

This research is funded by the University of Transport and Communications (UTC) under grant number T2026-CT-022. The authors would also like to thank their colleagues at the University of Transport and Communications, and the Vietnam Institute for Building Science and Technology, and FECON Corporation for their support in this work.

Declaration of Generative AI

During the preparation of this work, the authors do not use Generative AI and AI-assisted technologies tools in order to generate the content of the manuscript.

References

[1] B.O. Hardin, F.E. Richart. (1963). Elastic Wave Velocities in Granular Soils. *Journal of the Soil Mechanics and Foundations Division*, 89(1), 33–65. https://doi.org/10.1061/JSFEAQ.0000493

[2] B.O. Hardin, W.L. Black. (1966). Sand Stiffness Under Various Triaxial Stresses. *Journal of the Soil Mechanics and Foundations Division*, 92(2), 27–42. https://doi.org/10.1061/JSFEAQ.0000865

[3] T. Ohta, A. Hara, M. Niwa, T. Sakano. (1972). Elastic moduli of soil deposits estimated by N-values. *Proceedings of the 7th Annual Conference, The Japanese Society of Soil Mechanics and Foundation Engineering, pp. 265–268.*

[4] T. Imai, K. Tonoughi. (1982). Correlation of N value with S-wave velocity and shear modulus. *Penetration Testing, Volume 1. Routledge.* https://doi.org/10.1201/9780203743959-11

[5] H.B. Seed, I.M. Idriss, I. Arango. (1983). Evaluation of Liquefaction Potential Using Field Performance Data. *Journal of Geotechnical Engineering*, 109(3), 458–482. https://doi.org/10.1061/(ASCE)0733-9410(1983)109:3(458)

[6] P. Anbazhagan, T.G. Sitharam. (2010). Relationship between Low Strain Shear Modulus and Standard Penetration Test *N* Values. *Geotechnical Testing Journal*, 33(2), 150–164. https://doi.org/10.1520/GTJ102278

[7] M.N. Hussien, M. Karray. (2016). Shear wave velocity as a geotechnical parameter: an overview. *Canadian Geotechnical Journal*, 53(2), 252–272. https://doi.org/10.1139/cgj-2014-0524

[8] Japan International Cooperation Agency (JICA) and Vietnam Railways (VR). (2013). Study for the Formulation of High-Speed Railway Projects on Hanoi–Vinh and Ho Chi Minh–Nha

Trang Sections – Final Report, Volume I: Development of North-South Railways. *Japan International Cooperation Agency. Tokyo, Japan.*

[9] ASTM. (2017). ASTM D6913: Standard test methods for particle-size distribution (gradation) of soils using sieve analysis. *ASTM International.*

[10] ASTM. (2021). ASTM D7928-21: Standard test method for particle-size distribution (gradation) of fine-grained soils using sedimentation (hydrometer) analysis. *ASTM International.*

[11] ASTM. (2014). ASTM D7400-14: Standard test methods for downhole seismic testing. *ASTM International.*

[12] ABEM. (2011). User manual for Terraloc Pro. ABEM, Product No. 33 700 89.

[13] J.L. Östlund, A. Andersson, M. Ülker-Kaustell, J.-M. Battini. (2021). On the influence of shallow soil strata on the dynamic soil–structure interaction of simply supported high-speed railway bridges. *International Journal of Rail Transportation*, 9(5), 405–423. https://doi.org/10.1080/23248378.2020.1817804

[14] D.P. Connolly, K. Dong, P. Alves Costa, P. Soares, P.K. Woodward. (2020). High speed railway ground dynamics: a multi-model analysis. *International Journal of Rail Transportation*, 8(4), 324–346. https://doi.org/10.1080/23248378.2020.1712267

[15] J. Fernández-Ruiz, A. Castanheira-Pinto, P.A. Costa, D.P. Connolly. (2022). Influence of non-linear soil properties on railway critical speed. *Construction and Building Materials*, 335, 127485. https://doi.org/10.1016/j.conbuildmat.2022.127485

[16] K. Dong, D.P. Connolly, O. Laghrouche, P.K. Woodward, P.A. Costa. (2019). Non-linear soil behaviour on high speed rail lines. *Computers and Geotechnics*, 112, 302–318. https://doi.org/10.1016/j.compgeo.2019.03.028

[17] J.Y. Shih, D.J. Thompson, A. Zervos. (2017). The influence of soil nonlinear properties on the track/ground vibration induced by trains running on soft ground. *Transportation Geotechnics*, 11, 1–16. https://doi.org/10.1016/j.trgeo.2017.03.001

[18] X. Sheng, C.J.C. Jones, M. Petyt. (1999). Ground vibration generated by a harmonic load acting on a railway track. *Journal of Sound and Vibration*, 225(1), 3–28. https://doi.org/10.1006/jsvi.1999.2232

[19] W. Tengfei, L.N. Chau, T.B. Tien. (2025). Overview of advances and practices in high-speed railway earth structures in China. *Transport and Communications Science Journal*, 76(2025), 405–419. https://doi.org/10.47869/tcsj.76.2025.4